ANALYSIS OF EFFECTIVE CAPACITANCE OF ONE-PORT S-BAND GaN HEMT NON-FOSTER NEGATIVE-REACTANCE CIRCUIT

Akwuruoha, Charles Nwakanma
Department of Electrical and Electronic Engineering
Michael Okpara University of Agriculture Umudike
Umuahia, Nigeria
Email: akwuruoha.charles@mouau.edu.ng

ABSTRACT
This paper presents an analysis of the effective capacitance of one-port S-band gallium nitride high electron mobility transistor (GaN HEMT) non-Foster negative-reactance circuit. The analysis was carried out at S-band frequency ranges of 4.08 GHz to 4.11 GHz and 4.13 GHz to 4.17 GHz. The chosen frequency ranges are consistent with the frequency at which the simulated and fabricated non-Foster negative reactance circuit has negative reactance to frequency slope. The one-port non-Foster negative-reactance circuit was designed with Keysight Advanced Design System (ADS) Software and fabricated with FR_4 Microstrip substrate on printed circuit board with Copper conductor thickness of 1.5mm and measured with vector network analyzer (VNA). The circuit was designed with Cree CGHV4003F GaN HEMT biased with drain supply voltage of 20 V at quiescent drain-to-source (I_{DSq}) current of 19 mA. The one-port S-band non-Foster negative-reactance circuit has measured effective capacitance of -5 pF to -26 pF and simulated effective capacitance of -0.16 pF to -0.17 pF from 4.08 GHz to 4.11 GHz. The measured effective capacitance from 4.13 GHz to 4.17 GHz ranges from -20 pF to -53 pF as the simulated effective capacitance ranges from -0.18 pF to -0.21 pF. This one-port non-Foster negative reactance circuit showed effective negative capacitance at the chosen frequency ranges at measurement and simulation.

Keywords—one-port; non-Foster; negative-reactance circuit; GaN HEMT; S-band; effective capacitance

I. INTRODUCTION

One-port non-Foster negative-reactance circuits have the ability to improve the performance of microwave circuits by providing the needed negative reactance required to cancel out transistor parasitic capacitances which reduce circuit performance (Akwuruoha, 2018; Muller & Lucyszyn, 2015; Sterns, 2013; Kamat *et al.*, 2023). The non-Foster negative reactance circuits are usually negative capacitance circuits or negative inductance circuits. One-port non-Foster negative reactance circuit has one-port which serves as input impedance port and output impedance port. In this paper, the negative capacitance of one-port non-Foster negative reactance circuit at selected S-band frequency ranges of 4.08 GHz to 4.11 GHz and 4.35 GHz to 4.45 GHz was designed, fabricated, measured, simulated and investigated. Non-Foster negative reactance circuits have reportedly been used to enhance the performance of microwave circuits such as antennas (Elfrgani & Rojas, 2015; Sussman-Fort & Rudish, 2009; Nagarkoti *et al.*, 2014; Haskou *et al.*, 2017; Hansen, 2003; Jacob *et al.*, 2014; Koulouridis & Volakis, 2009), meta-materials (Barbuto et al, 2013; Mirzaei & Eleftheriades, 2011) and power amplifiers (Lee *et al*, 2015; Ghadiri & Moez, 2010; Ledezma, 2015; Akwuruoha *et al.*, 2017; Akwuruoha & Hu, 2017). To the best of the author's knowledge, this is the first reported analysis of the effective negative capacitance of one-port non-Foster negative reactance circuit at S-band frequencies of 4.08 GHz to 4.11 GHz and 4.35 GHz to 4.45 GHz. This paper is divided into five sections as follows. Section II discusses non-Foster circuit theory and types. Section III discusses materials and methods. Section IV discusses the measurement and simulation results. Section V concludes the paper.

II. NON-FOSTER NEGATIVE REACTANCE CIRCUIT THEORY

Non-Foster negative reactance circuit reflection coefficient moves in counter-clockwise direction with respect to frequency on a Smith Chart (Sussman-Fort & Rudish, 2009; Muller & Lucyszyn, 2015). Non Foster negative reactance circuits are classified into two depending on the type of impedance conversion associated with the circuit. Non-Foster negative reactance circuits are either negative impedance converters (NIC) or negative impedance inverters (NII). Non-Foster negative reactance circuits are further classified as open circuit stable (OCS) and short circuit stable (SCS) (Akwuruoha et al, 2017). The driving-point impedance of non-Foster negative reactance circuit is equal to the negative value of the load impedance. The load impedance is related to the input impedance by (Akwuruoha, 2018)

$$Z_{in} = -KZ_L \quad (1)$$

Where Z_{in} is the input impedance, K is the impedance converter coefficient and Z_L is the load impedance. The derivative of the reactance and the susceptance of the non-Foster negative reactance circuit with respect to angular frequency are negative (Muller & Lucyszyn, 2015)

$$\frac{dX}{d\omega} < 0 \quad (2)$$

$$\frac{dB}{d\omega} < 0 \quad (3)$$

where X is reactance, B is susceptance and ω is angular frequency.

The driving-point impedance of a non-Foster negative reactance circuit depends on the load impedance terminating the circuit as well as circuit properties which are defined in accordance with a hybrid parameter network whereby the input/output currents (I_1/I_2) are related to the input/output voltages (V_1/V_2) by

$$\frac{V_1}{I_1} = \frac{V_2}{I_2} \quad (4)$$

The equivalent circuits of the linear two-port networks are shown in Figures 1 and 2 while the h-parameter equivalent circuit is shown in Figure 3.

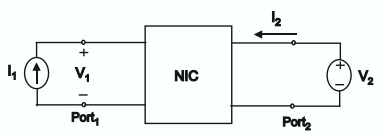

Figure 1. NIC as a linear two-port

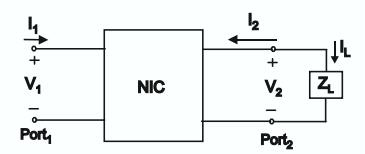

Figure 2. NIC as a linear two-port network with arbitrary passive

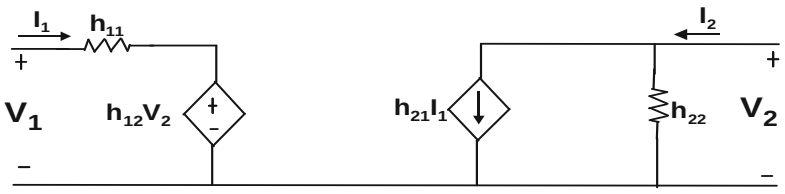

Figure 3. Two-port h-parameter equivalent

The h-parameter equations are given by (Akwuruoha, 2018)

$$V_1 = h_{11}I_1 + h_{21}V_2 \quad (5)$$

$$V_2 = h_{21}I_1 + h_{22}V_2 \quad (6)$$

When the input port is on open circuit ($I_1 = 0$) and the output port is on short circuit ($V_2=0$), the h-parameters: h_{11}, h_{12}, h_{21} and h_{22} are respectively given by

$$h_{11} = \frac{V_1}{I_1} \qquad (V_2 = 0) \tag{7}$$

$$h_{12} = \frac{V_1}{V_2} \qquad (I_1 = 0) \tag{8}$$

$$h_{21} = \frac{I_2}{I_1} \qquad (V_2 = 0) \tag{9}$$

$$h_{22} = \frac{I_2}{V_2} \qquad (I_1 = 0) \tag{10}$$

where h_{11} is the input impedance when port 2 is on short circuit and h_{22} is the output admittance when port 1 is on open circuit. The h_{12} and h_{21} are dimensionless voltage and current ratios. The h_{12} is the reverse voltage ratio when port 1 is on open circuit while h_{21} is the forward transmission current gain when port 2 is on short circuit. If an arbitrary passive load Z_L is terminated across the output port, the driving-point impedance seen looking into the input port is given by

$$Z_{in} = h_{11} - \left[\frac{(h_{12}h_{21}Z_L)}{(h_{22}Z_L+1)}\right] \tag{11}$$

For an ideal negative impedance converter,

$$Z_{in} = -Z_L \tag{12}$$

To realize (12) from (11), the necessary conditions are:

$$h_{11} = 0 \tag{13}$$

$$h_{22} = 0 \tag{14}$$

$$h_{12}h_{21} = 1 \tag{15}$$

(13), (14) and (15) are true regardless of if the output terminal pairs are interchanged by terminating the arbitrary passive load Z_L to port1 or port 2. The impedance converter coefficient (K) of negative impedance converter is given by

$$K = h_{12}h_{21} > 0 \tag{16}$$

III. MAERIALS AND METHODS

A. Materials

The materials are Keysight Advanced Design System Software (ADS), Vector Network Analyzer (VNA) and Fr_4 Microstrip substrate.

B. Methods

The One-port non-Foster negative reactance circuit was designed based on Cree's CGHV40030F gallium nitride high electron mobility transistors (GaN HEMTs) biased with drain supply voltage of 20V at quiescent drain-to-source current of 19mA as shown in Figure 4. The circuit consists of microstrip lines, inductors and capacitors. The width and length of the Microstrip lines are in millimeters. The circuit was fabricated on printed circuit board using Fr_4 microstrip substrate with dielectric constant of 4.6 and copper conductor with thickness of 1.5mm. The schematic circuit and the snapshot are shown in Figures 5 and 6 respectively.

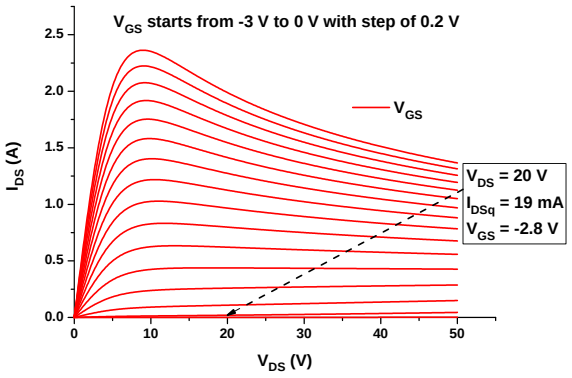

Figure 4. DC I-V characteristic bias

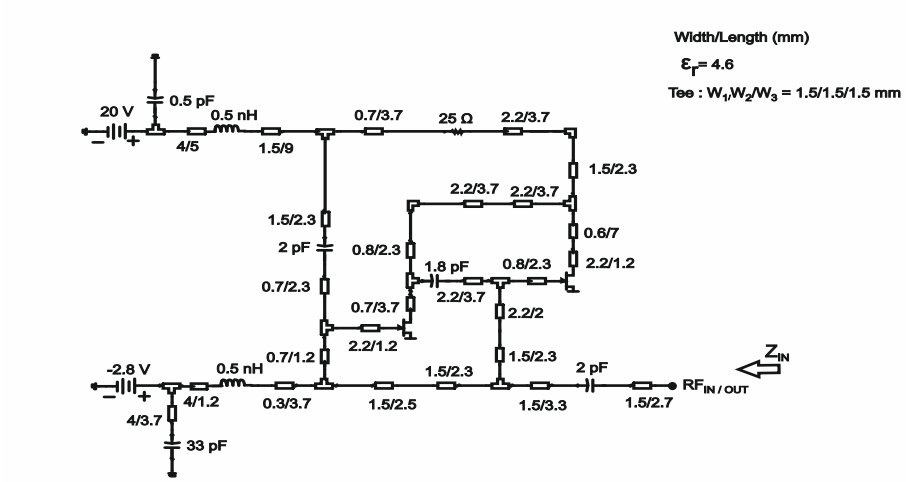

Figure 5. One-port non-Foster negative reactance circuit

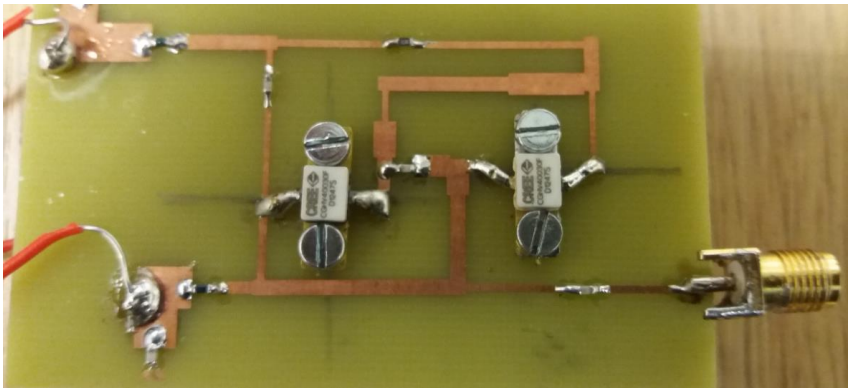

Figure 6 Snapshot of the PCB fabricated one-port non-Foster negative reactance

IV. RESULTS AND DISCUSSION

The measurement and simulation of the unbalanced non-Foster negative reactance circuit were carried out in two instances. In the first instance, the measurement and simulation were carried out from 4.08 GHz to 4.11 GHz whereas in the second instance, the measurement and simulation were carried out from 4.13 GHz to 4.17 GHz. The chosen frequency ranges are consistent with the frequency at which the simulated and fabricated non-Foster negative reactance circuit has negative reactance to frequency slope.

In the first instance, the non-Foster negative reactance circuit was measured and simulated from 4.08 GHz to 4.11 GHz and the results are shown in Figures 7 and 8. The graph of magnitude and imaginary part of input impedance versus frequency from 4.08 GHz to 4.11 GHz shown in Figure 7 indicates that the circuit has negative reactance to frequency slope across the 300 MHz bandwidth. The measured effective capacitance from 4.08 GHz to 4.11 GHz ranges from -5 pF to -26 pF whereas the simulated effective capacitance ranges from -0.164 pF to -0.172 pF as shown in Figure 8.

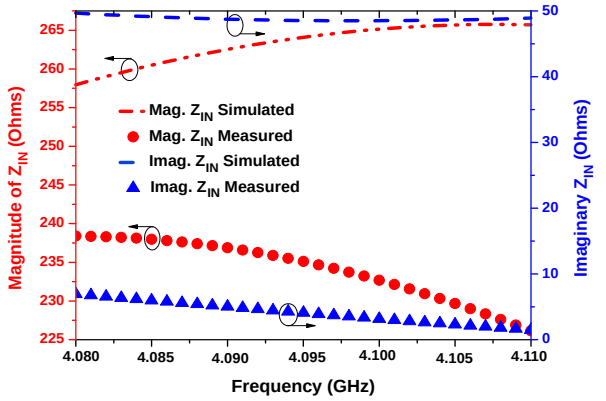

Figure 7. Magnitude and Imaginary part of input impedance from 4.08 to 4.11 GHz

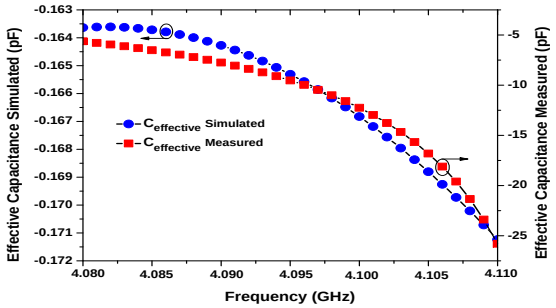

Figure 8. Effective capacitance from 4.08 to 4.11 GHz

In the second instance, the non-Foster negative reactance circuit was measured and simulated from 4.13 GHz to 4.17 GHz as shown by the result in Figures 9 and 10. The graph of magnitude and imaginary part of input impedance versus frequency from 4.13 GHz to 4.17 GHz shows negative reactance to frequency slope across the 400 MHz bandwidth as shown in Figure 9. The measured effective negative capacitance ranges from -20 pF to -53 pF whereas the simulated effective negative capacitance ranges from -0.18 pF to -0.21 pF as shown in Figure 10.

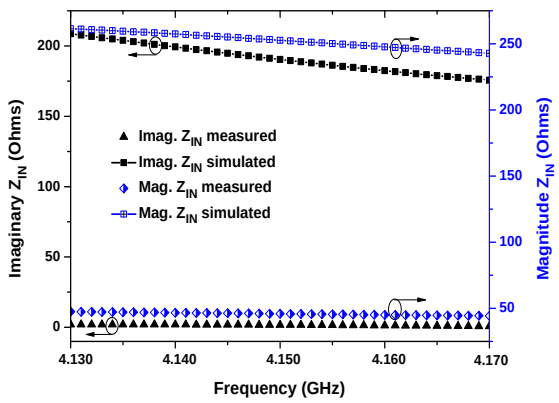

Figure 9. Magnitude and Imaginary part of input impedance from 4.13 to 4.17 GHz

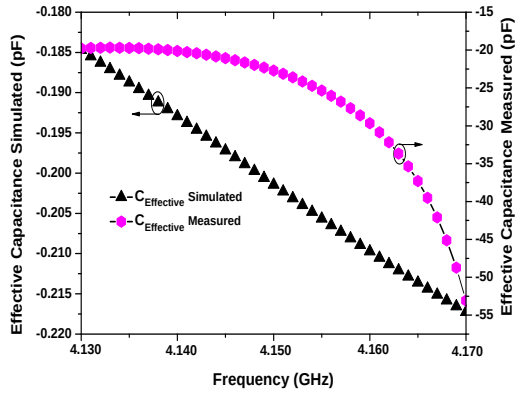

Figure 10. NFC Effective capacitance from 4.13 to 4.17 GHz

V. CONCLUSION

One-port GaN HEMT non-Foster negative reactance circuit have been designed, simulated, fabricated and measured at S-band frequency ranges of 4.08 GHz to 4.11 GHz and 4.13 GHz to 4.17 GHz. The results indicate that the fabricated and simulated non-Foster circuit consistently showed negative reactance to frequency slope across the bandwidth and good effective negative capacitance. One-port non-Foster negative reactance circuit can find applications in microwave circuit where there is desirability to use the effective negative capacitance to cancel out parasitic capacitances and enhance circuit performance**.**

.

ACKNOWLEDGMENT

The author is grateful to Cree Incorporations USA for providing the model used in this work and The University of Manchester UK Microwave Laboratory for carrying out the measurement.

REFERENCES

Akwuruoha, C. N. (2018). Modelling and Design of Non-Foster Class-J Power Amplifier for Wireless Communication Systems.PhD Dissertation, The University of Manchester, Manchester, United Kingdom.

Akwuruoha, C. N., Hu, Z. & Licea, Y. J. (2017). Microstrip non-foster circuit high efficiency high power class-J GaN HEMT amplifier. IEEE Conference on Microwaves, Antennas, Communications and Electronic Systems, Tel-Aviv, Israel,1-4.

Akwuruoha, C. N. & Hu, Z. (2017). 64 to 70 GHz Microstrip Non-Foster Circuit Class-J GaAs pHEMT power amplifier. 25th Telecommunication Forum, Belgrade, Serbia, 1-4.

Barbuto, M., Monti, A., Bilotti, F. & Toscano, A. (2013). Design of a Non-Foster Activity Loaded SRR and Application in Metamaterial-Inspired Components. *IEEE Transactions on Antennas and Propagation*, 61(3), 1219-1227.

Elfrgani, A. M. & Rojas, R. G. (2015). "Successful Realization of Non-Foster Circuits for Wide-Band Antenna Applications," IEEE MTT-S International Microwave Symposium, Phoenix, AZ, USA, 1-4.

Ghadiri, A. & Moez, K. (2010). Gain-Enhanced Distributed Amplifier using Negative Capacitance. *IEEE Transactions on Circuits and Systems*, 57(11), 2834-2843.

Hansen, R. C. (2003). Dipole arrays with non-foster circuits. IEEE International Symposium on Phase Array Systems and Technology, Boston, MA, USA, 40-44.

Haskou, A., Lemurs, D., Collardey, S. & Sharaiha, A. (2017). A non-foster circuit design for antenna miniaturization. International Symposium on Antennas and Propagation, Okinawa, Japan, 286-287.

Jacob, M. M., Long, J. & Sievenpiper, D. F. (2014). Non-Foster Loaded Parasitic Array for Broadband Steerable Patterns. *IEEE Transactions on Antenna and Propagation*, 62(12), 6081-6090.

Kamat, J., Lin, C., Arora, P., & Gupta, S. (2023). A Review of CMOS Non-Foster Circuits. International Symposium on Circuits and Systems, Monterey, CA, USA, 1-5.

Koulouridis, S., & Volakis, J. Y. (2009). Non-Foster Circuits for Small broadband Antennas. 2009 IEEE Antennas and Propagation Society International Symposium, North Charleston, SC, USA, 1-4.

Ledezma, L. M. (2015). Doherty power amplifier with lumped non-foster impedance inverter. International Symposium on Wireless and Microwave Circuit and Systems, Waco, Texas USA, 1-4.

Lee, S., H. Park, H., J. Kim, J. & Y. Kwon, Y. (2015). A 6-18 GHz GaN pHEMT Power Amplifier Using Non-Foster matching. IEEE MTT-S International Microwave Symposium, Phoenix, AZ, USA, 1-4.

Mirzaei, H. & Eleftheriades, G. V. (2011). A Wideband Metamaterial-Inspired Compact Antenna Using Embedded Non-Foster Matching. IEEE International Symposium on Antennas and Propagation, Spoken, WA, USA, 1950-1953.

Muller, A. A. & S. Lucyszyn, S. (2015). Properties of purely reactive Foster and non-Foster passive networks. *Electronic Letters*, 51 (23), 1882-1884.

Nagarkoti, D. S., Rajah, K. Z. & Hao, Y. (2014). Design and Stability of Negative Impedance Circuits for Non-Foster Matching of a Monopole Antenna. Proceedings of 8th European Conference on Antennas and Propagation, The Hague, Netherlands, 2707-2709.

Sterns, S. D. (2013). Circuit Stability Theory for Non-Foster Circuits. Proceedings of IEEE MTTS-S International Microwave Symposium, Seattle, WA, USA, 1-3.

Sussman-Fort, S. E. & Rudish, R. M. (2009). Non-Foster Impedance Matching of Electrically-Small Antennas. *IEEE Transactions on Antennas and Propagation*, 57(8), 2230-2241.